

RSC Advances



This is an *Accepted Manuscript*, which has been through the Royal Society of Chemistry peer review process and has been accepted for publication.

Accepted Manuscripts are published online shortly after acceptance, before technical editing, formatting and proof reading. Using this free service, authors can make their results available to the community, in citable form, before we publish the edited article. This *Accepted Manuscript* will be replaced by the edited, formatted and paginated article as soon as this is available.

You can find more information about *Accepted Manuscripts* in the [Information for Authors](#).

Please note that technical editing may introduce minor changes to the text and/or graphics, which may alter content. The journal's standard [Terms & Conditions](#) and the [Ethical guidelines](#) still apply. In no event shall the Royal Society of Chemistry be held responsible for any errors or omissions in this *Accepted Manuscript* or any consequences arising from the use of any information it contains.



Journal Name

ARTICLE

Anchoring ternary CuFePd nanocatalysts on reduced graphene oxide to improve the electrocatalytic activity for the methanol oxidation reaction

Received 00th January 20xx,
Accepted 00th January 20xx

DOI: 10.1039/x0xx00000x

www.rsc.org/

Xuan Zhang*, Jia-Wei Zhang†, Bei Zhang†

Ternary CuFePd nanocatalysts were anchored on reduced graphene oxide (rGO) by a simple one-pot chemical reduction with NaBH₄ at room temperature, served as a novel CuFePd/rGO electrocatalyst toward methanol oxidation reaction (MOR). The CuFePd/rGO nanocatalysts were characterized by transmission electron microscopy (TEM), X-ray diffraction (XRD), X-ray photoelectron spectroscopy (XPS), energy dispersive X-ray spectroscopy (EDS), as well as inductively coupled plasma atomic emission spectroscopy (ICP-AES). The electrocatalytic performance for MOR was evaluated by cyclic voltammetry. It was found that the as-prepared ternary CuFePd/rGO exhibited improved activity and stability in comparison with Pd/rGO and binary CuPd/rGO, FePd/rGO, respectively. Furthermore, the effect of composition ratio of Cu to Fe on the electrocatalytic performance was also discussed.

1. Introduction

The extensive utilization of fossil fuels as energy sources has caused a worldwide environmental contaminant and global warming. Thus the exploring of the renewable and clean energy source has become an urgent task. Recently, direct methanol fuel cells (DMFCs), as a typical promising sustainable power source, has drawn increasing attention due to its unique advantages, such as high power density, low pollutant emission, cheap price of fuel, portability and low operating temperature.^{1–4} However, the relatively poor methanol oxidation kinetics significantly blocks the practical application of DMFCs. To a large extent, the electrochemical performance in fuel cells primarily depends on anode electrocatalysts.^{5–7} It has been well-known that Pt-based catalyst is one of the most efficient and extensively used catalysts in DMFCs due to its extraordinary electric activity and chemical stability.^{7,8} However, Pt-based catalysts still have some disadvantages such as their high cost due to the limit supply of Pt, and serious kinetic constraints from CO poisoning.^{9–11} Alternatively, Pd, whose abundance is at least fifty times more than that of Pt on earth, could serve as a good candidate for the methanol oxidation reaction (MOR) under alkaline conditions.^{12–15} Nevertheless, the electrocatalytic activity and stability of pure Pd nanoparticles are still not satisfied for the practical application in fuel cells technology, due to the low utilization efficiency of Pd, where only outmost Pd atom can direct contact with methanol and perform the electrocatalytic

activity. Therefore, the developing of high efficient Pd-based anode catalysts is highly desired.

One approach to improve the performance is the tuning of electronic structures of Pd by forming the bimetallic structures with a second noble metal, such as Ru, Au and Rh.^{16–20} Most promisingly, combining Pd with non-noble metals could improve the catalytic activity but also reduce the cost of the catalysts. For example, Ni@Pd core-shell nanoparticles supported on multi-walled carbon nanotubes have showed a high electrocatalytic activity and stability in comparison with pure Pd counterpart.²¹ Furthermore, ternary metallic catalysts have been considered more efficient in comparison with the binary one in DMFCs.^{22,23}

In addition, it has been recognized that support materials could also play a crucial role in performance of electrocatalyst via a support-catalyst interaction.^{24,25} An ideal catalyst support should have: i) high specific surface area to achieve high metal dispersion; ii) good electric conductivity to promote fast electron transfer in redox reactions; iii) high stability to maintain a stable catalyst structure; iv) strong affinity to immobilize catalyst nanoparticles.^{26,27} Carbon materials, such as carbon black,²⁸ carbon nanospheres,²⁹ carbon nanotubes,^{30–32} fullerene,^{33–35} and graphene,^{36–38} have been considered to be potential support materials. Graphene, a unique two-dimensional carbon material, has received much attention on utilization as novel support materials due to its large surface areas and high electrical conductivity.^{39–41} Especially reduced graphene oxide (rGO), holding many residual epoxides, hydroxides and carboxylic acid groups that endows much advantages such as providing anchor sites for metal nanoparticles, became more popular in support materials.^{42–45}

College of Chemistry, Chemical Engineering & Biotechnology, Donghua University, Shanghai 201620, China.

† These authors contributed equally.

*Corresponding Author: xzhang@dhu.edu.cn

In this work, a novel CuFePd/rGO electrocatalyst, ternary CuFePd nanocatalysts were anchored on reduced graphene oxide (rGO), was developed by a simple one-pot chemical reduction with NaBH₄ at room temperature. The as-prepared CuFePd/rGO exhibited improved activity and stability in comparison with Pd/rGO and binary CuPd/rGO, FePd/rGO, respectively. Furthermore, the effect of composition ratio of Cu to Fe on the electrocatalytic performance was also discussed.

2. Experimental section

Graphite powder (99.85%) and Nafion (5%) were purchased from XFNANO (Nanjing, China) and Alfa, respectively. Palladium chloride (PdCl₂), copper sulfate pentahydrate (CuSO₄·5H₂O), iron sulfate heptahydrate (FeSO₄·7H₂O), potassium permanganate (KMnO₄), hydrogen peroxide (H₂O₂, 30%), concentrated sulfuric acid (98%, H₂SO₄), and concentrated nitric acid (HNO₃, 65%) were obtained from Sinopharm Chemical Reagent Corp. (Shanghai, China). All chemicals were analytical grade and used as received.

X-ray diffraction (XRD) and X-ray photoelectron spectroscopy (XPS) measurements were performed on Rigaku D/max 2550 with Cu-Kα radiation and PHI 5400, respectively. Transmission electron microscope (TEM) and energy dispersive X-ray spectroscopy (EDS) were carried out on JEM-2100F. Inductively coupled plasma atomic emission spectroscopy (ICP-AES) was measured on Leeman ICP-AES Prodigy.

Graphene oxide (GO) was prepared according to a modified Hummers method.^{46,47} In brief, graphite powder (0.5 g) was treated with concentrated acid (1.5 mL HNO₃ and 15 mL H₂SO₄) under an ice-water bath and KMnO₄ (2 g) was slowly added into the mixture solution within 20 min and warmed to 45 °C for another 1 h. Then water (25 mL) was added and the temperature was raised to 90 °C for 30 min. Finally, the solution was cooled down to room temperature and diluted with water (60 mL), followed by addition of H₂O₂ (2 mL, 30%) within 30 min. The GO was obtained by centrifugation, washing with water, and drying in vacuum at 40 °C.

Ternary CuFePd/rGO catalysts were synthesized in a one-pot procedure at ambient temperature. Briefly, GO (20 mg) was dissolved in deionized water (30 mL) under ultrasonication for 0.5 h to obtain a homogeneous solution. FeSO₄ (160 μL, 0.4 M) and freshly prepared NaBH₄ (5 mL, 0.1M) were sequentially dropped into the above GO solution. CuSO₄ (160 μL, 0.4 M) and NaBH₄ (5 mL, 0.1 M) were then sequentially dropped into the above mixture, followed by the addition of PdCl₂ (6.4 mL, 0.01 M) and NaBH₄ (5 mL, 0.1 M), respectively. Finally, another NaBH₄ (5 mL, 0.1 M) was dropped into the above mixture and stirred overnight. The ternary CuFePd/rGO catalysts was obtained by centrifuging, washing 3 times with deionized water and ethanol, and finally drying at 50 °C overnight. For a comparison, ternary CuFePd/rGO with different ratio of Cu to Fe, binary FePd/rGO and CuPd/rGO as well as pure Pd/rGO catalysts were also prepared under the same procedure with different metal precursor.

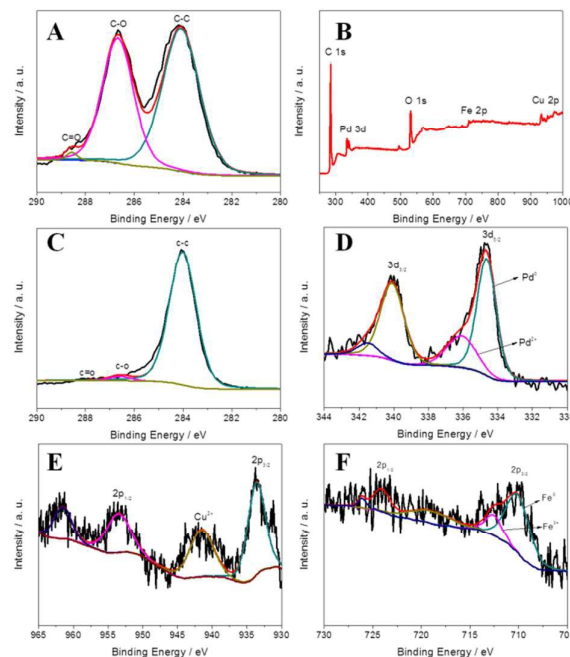


Fig. 1 XPS spectra of GO C1s (A), CuFePd/rGO (B), rGO C1s (C), Pd 3d (D), Cu 2p (E) and Fe 2p (F).

The electrochemical measurements, including cyclic voltammetry (CV) and chronoamperometry (CA), were carried out on a CHI 660D electrochemical workstation (CH Instruments, Inc, Shanghai) at ambient temperature. The counter and reference electrodes were a platinum wire and a saturated calomel electrode (SCE), respectively. The working electrode was prepared as described below. The as-prepared catalyst (2 mg) was ultrasonically dispersed in 1.0 mL ethanol solution for 0.5 h, and the ink (5 μL) was transferred onto a glassy carbon that was pre-polished sequentially with 0.3 and 0.05 mm alumina oxide powder, followed by coating Nafion solution (5 μL, 0.5%) and drying at ambient temperature. The as-prepared working electrode was then activated by CV in 1.0 M H₂SO₄ under a potential window of -0.2 to 1.0 V (vs. SCE) with a scan rate of 50 mV S⁻¹. The electrocatalytic activities of catalysts for methanol oxidation reaction were performed by CV in 1.0 M NaOH solution containing 1.0 M MeOH under a potential window of -1.0 to 0.2 V (vs. SCE) with a scan rate of 50 mV S⁻¹. The stability was examined by CA at a potential of -0.2 V for 6000 s.

3. Result and discussion

3.1. Characterization of electrocatalyst

The XPS spectra of GO and CuFePd/rGO were shown in Fig. 1. The C1s band could be deconvoluted into three main peaks centered at 284.08, 286.68 and 288.58 eV, corresponding to the alkyl C and sp²-bonded carbon network (C-C/C=C), the hydroxyl and epoxy groups (C-O), and the carbonyl C (C=O),

respectively. The peak intensity ratio of C-C to C-O in the rGO spectra obviously increased in comparison to that of GO (Figs. 1A and 1C), indicating that the GO has been largely changed into rGO with NaBH_4 as reductant. In addition, the peaks of Pd, Cu and Fe were also observed in XPS spectra and could be deconvoluted into Pd $3d_{5/2}$ and $3d_{3/2}$, Cu $2p_{1/2}$ and $2p_{3/2}$, Fe $2p_{1/2}$, $2p_{3/2}$ peaks, respectively (Figs. 1B–1F).^{4,48–50} This indicates that CuFePd/rGO were successfully fabricated.

Fig. 2 showed the XRD patterns of as-prepared electrocatalysts. The four diffraction peaks could be assigned to (111), (200), (220) and (311) planes of the crystalline face centered cubic (fcc) structure of Pd, respectively. The average crystallite size (D) was then estimated to be 3–5 nm from the (111) diffraction peak by Scherrer's equation:

$$D = \frac{0.9\lambda}{B\cos\theta}$$

where D is the mean particle size in nm, λ is 0.1542 nm for $\text{CuK}\alpha$, B is the full width at half maximum (FWHM) of the diffraction peak in radians, and θ is the Bragg angle. Notably, the diffraction peaks of CuFePd/rGO, CuPd/rGO and FePd/rGO slightly shifted to higher angles in comparison with Pd/rGO, likely due to the incorporation of Cu and Fe into the Pd lattice.

The as-prepared CuFePd/rGO catalysts were then characterized by TEM and EDS. The representative TEM images were shown in Fig. 3A–C. It is clear that the catalyst nanoparticles are uniformly dispersed on rGO surface with a mean size of 3–5 nm, in a good agreement with the value estimated from XRD. From high-resolution TEM (HR-TEM) image of CuFePd/rGO catalysts, the fringe spacing of 0.224 nm was revealed (inset in Fig. 3B), close to the lattice space of (111) plane fcc structure of Pd. An observation of clear SAED pattern indicates the crystalline nature of Pd (inset in Fig. 3A). As shown in Fig. 3D, the EDS analysis clearly showed the signals of Cu, Fe and Pd in as-prepared CuFePd/rGO catalysts, where the elements of C and O could originate from graphene support. The Pd loading was further determined by ICP-AES to be 24–26% for the ternary CuFePd/rGO, binary FePd/rGO and CuPd/rGO as well as mono-metallic Pd/rGO, respectively. The little higher loading of Pd on these catalysts than the expected theoretical value of 20% could be attributed to the loss of graphene in the preparation process. On the other hand, the mass fractions of Cu and Fe in CuFePd/rGO were found to be 11 and 9.3% respectively, in good agreement with the expected values from the precursors concentration used. These results supported that the ternary CuFePd nanocatalysts were successfully anchored on the graphene sheets.

3.2. Electrocatalytic performance

To demonstrate the electrocatalytic performance of the as-prepared CuFePd/rGO catalyst towards the MOR, the CV measurements were conducted in 1 M H_2SO_4 and 1 M $\text{NaOH} + 1.0$ M MeOH solutions respectively. Fig 4 presents the cyclic voltammetry profiles of CuFePd/rGO, FePd/rGO, CuPd/rGO and Pd/rGO in 1 M H_2SO_4 . The electrochemical surface area

(ECSA) was estimated by calculating the charges accumulated during hydrogen desorption according to the follows equation:

$$ECSA = \frac{Q}{km}$$

where, Q (μC) is the integrated charge from the hydrogen desorption region by excluding the double electric layer; k is $210 \mu\text{C cm}^{-2}$, corresponding the charge density for monolayer of Pd from the adsorption/desorption of hydrogen; and m is the catalysts amount.⁵¹ It was found that the ECSA was estimated to be 43.5, 32.6, 28.3 and $9.70 \text{ m}^2 \text{ g}^{-1}$ for CuFePd/rGO, FePd/rGO, CuPd/rGO and Pd/rGO, respectively. The ECSA was also measured from the electric charge of reduction of monolayer Pd oxide with an assumption of $424 \mu\text{C cm}^{-2}$,⁵² and the corresponding value was estimated to be 46.4, 38.2, 36.5 and $13.7 \text{ m}^2 \text{ g}^{-1}$, respectively. The larger ECSA value of CuFePd/rGO suggested that the ternary metallic catalyst could have more active sites compared to the binary and mono-metallic counterparts.

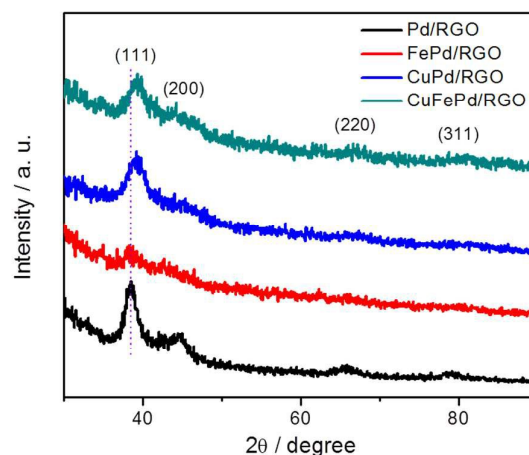


Fig. 2 XRD patterns of Pd/rGO, FePd/rGO, CuPd/rGO and CuFePd/rGO catalysts.

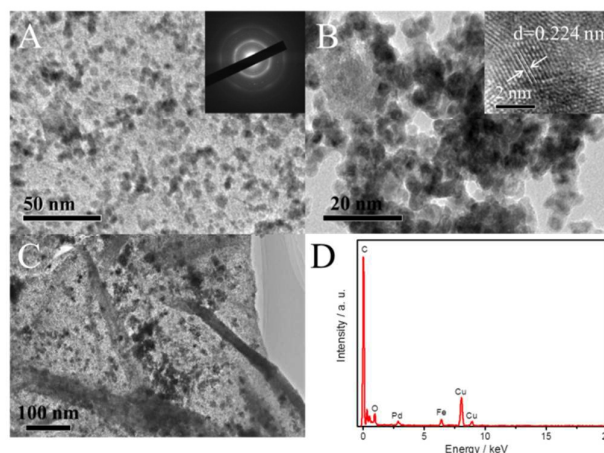


Fig. 3 TEM images (A–C) and EDS analysis (D) of CuFePd/rGO. Insets are SAED pattern (A) and magnified HR-TEM image (B).

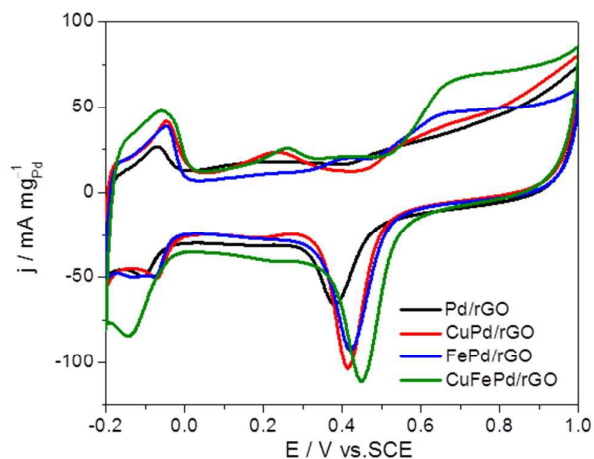


Fig. 4 CV curves of Pd/rGO, CuPd/rGO, FePd/rGO and CuFePd/rGO catalysts in 1 M H_2SO_4 solution with a scan rate of 50 mV s^{-1} .

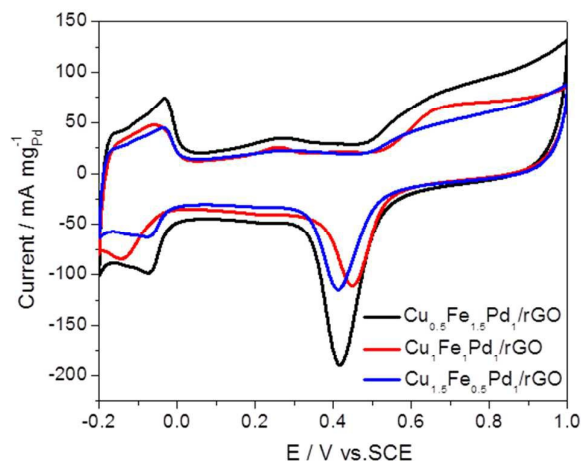


Fig. 7 CV of CuFePd/rGO catalysts with various ratio of Cu to Fe in 1 M H_2SO_4 solution with a scan rate of 50 mV s^{-1} .

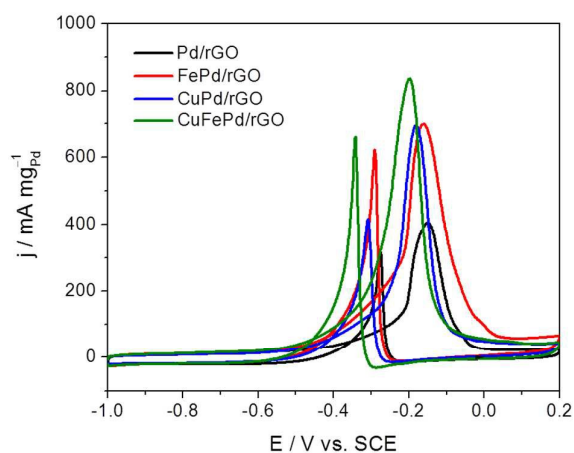


Fig. 5 CV of Pd/rGO, FePd/rGO, CuPd/rGO, and CuFePd/rGO catalysts in 1 M NaOH + 1 M MeOH solution with a scan rate of 50 mV s^{-1} .

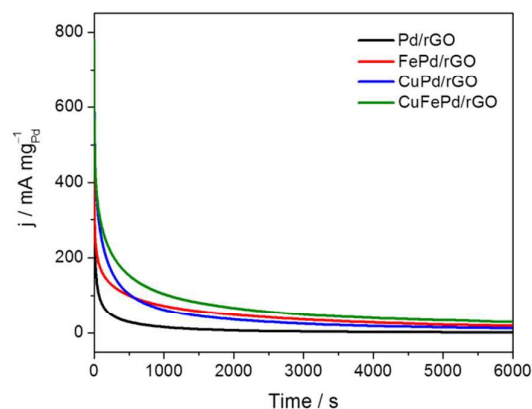


Fig. 6 CA curves of Pd/rGO, FePd/rGO, CuPd/rGO and CuFePd/rGO catalysts in 1 M NaOH + 1 M MeOH solution at -0.2 V .

The cyclic voltammograms of CuFePd/rGO, FePd/rGO, CuPd/rGO and Pd/rGO for the MOR in 1 M NaOH + 1.0 M MeOH solutions are shown in Fig. 5. The peaks in the forward scans correspond to methanol oxidation, whereas the peaks in the backward scans are attributed to the removal of incompletely oxidized CO-like carbonaceous species.¹² The mass activity of CuFePd/rGO for MOR was found to be 835 mA mg^{-1} , higher than those of FePd/rGO (697 mA mg^{-1}), CuPd/rGO (697 mA mg^{-1}) as well as Pd/rGO (406 mA mg^{-1}), respectively. This clearly demonstrates an enhanced catalytic activity on the CuFePd/rGO, likely due to the presence of dopant Cu and Fe not only increased the utilization efficiency, but also lowering the d-band center of Pd and thereby altering the electronic properties of the overall catalyst.^{16–21,53} As a result, the coverage of CO-like carbonaceous species on Pd surface was reduced that make more active site for MOR available, resulting from the diminished affinity toward CO due to the presence of defect sites at interconnects between Pd and dopant Cu/Fe segments.⁵³ It can be noted that the onset potential of CuFePd/rGO was more negative than those of others, revealing that the methanol is easier to be oxidized on the ternary alloyed catalyst.

The stability of these catalysts was evaluated by CA at -0.2 V in 1 M NaOH + 1 M MeOH solution for 6000 s (Fig. 6). It can be seen that the currents of all the catalysts initially decayed and then reached a steady state. Overall, the ternary CuFePd/rGO catalyst maintained the highest steady state current density over the whole time region of 6000 s than the corresponding binary CuPd/rGO and FePd/rGO as well as mono-metallic Pd/rGO, respectively. This suggested that the as-prepared ternary CuFePd/rGO catalyst holds an enhanced stability for MOR.

To further gain insights into the influence of chemical composition on electrocatalytic performance, ternary catalysts $\text{Cu}_{0.5}\text{Fe}_{1.5}\text{Pd}_1/\text{rGO}$ and $\text{Cu}_{1.5}\text{Fe}_{0.5}\text{Pd}_1/\text{rGO}$ with various precursor ratio of Cu to Fe, were prepared and their electrocatalytic performances for MOR were compared with that of

CuFePd/rGO. It was found that the change of metal composition ratio could tune the electrocatalytic performance toward MOR. As shown in Fig. 7, the ECSA was estimated to be 58.6, 43.5, and 34.6 $\text{m}^2 \text{g}^{-1}$ for $\text{Cu}_{0.5}\text{Fe}_{1.5}\text{Pd}_1/\text{rGO}$, $\text{Cu}_1\text{Fe}_1\text{Pd}_1/\text{rGO}$, and $\text{Cu}_{1.5}\text{Fe}_{0.5}\text{Pd}_1/\text{rGO}$ catalysts, respectively. The CV recorded in 1 M NaOH solution containing 1 M MeOH showed the highest forward peak current density on CuFePd/rGO among these ternary catalysts (Fig. 8). Additionally, the CA curves recorded at -0.2 V revealed that CuFePd/rGO also holds the highest steady state current density for MOR (Fig. 9). These results suggested that a fine tailoring of the chemical composition in ternary metallic catalyst could efficiently tune the electrocatalytic performance.

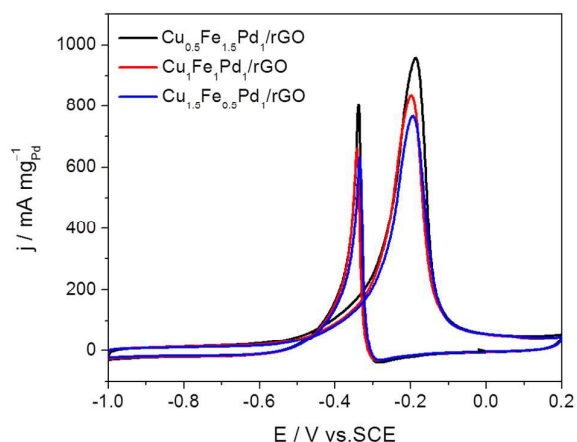


Fig. 8 CV curves of CuFePd/rGO catalysts with various ratio of Cu to Fe in 1 M NaOH + 1 M MeOH solution with a scan rate of 50 mV s^{-1} .

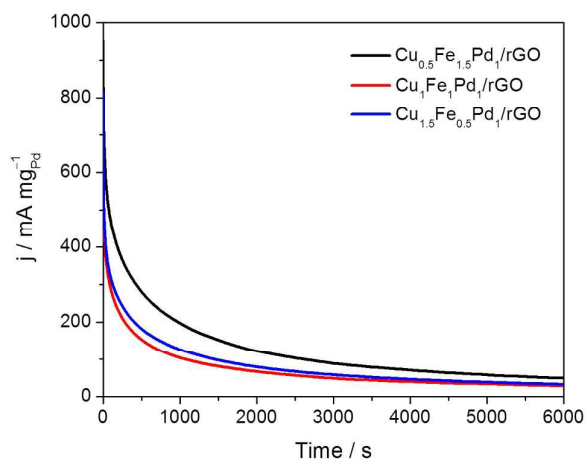


Fig. 9 CA curves of CuFePd/rGO catalysts with various ratio of Cu to Fe in 1 M NaOH + 1 M MeOH solution at -0.2 V .

4. Conclusion

In conclusion, ternary CuFePd nanocatalysts were anchored on graphene by a simple one-pot chemical reduction with NaBH_4 at room temperature, served as a novel CuFePd/rGO electrocatalyst toward MOR. Compared with the binary CuPd/rGO and FePd/rGO, and mono-metallic Pd/rGO, the as-prepared ternary electrocatalyst CuFePd/rGO displayed a substantially enhanced activity and improved stability for MOR. This could be attributed to the synergistic interactions between Pd and dopant metals Cu and Fe, as well as catalyst and graphene support. The electrocatalytic performance were found to be dependent on chemical composition ratios of dopant Cu and Fe in CuFePd/rGO, suggesting that fine tailoring of the chemical composition in ternary metallic catalyst could efficiently tune the electrocatalytic performance. These findings provide a straightforward one-pot synthesis strategy and insights into designing novel high-performance and cheap Pd-based catalysts for MOR in fuel cells.

Acknowledgements

This work was financially supported by Fundamental Research Funds for the Central Universities (Nos. EG2015020, 2232014D3-11, 2232015G1-61).

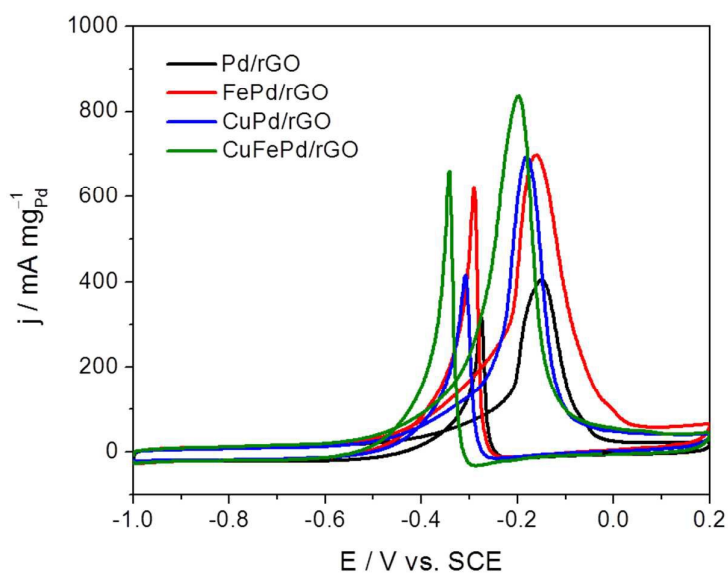
Notes and references

- J.N. Tiwari, R.N. Tiwari, G. Singh and K.S. Kim, *Nano Energy* 2013, 2, 553–578.
- H.S. Liu, L.J. Song, L. Zhang, J.J. Zhang, H.J. Wang and D.P. Wilkinson, *J. Power Sources* 2006, 155, 95–110.
- B. Singh, L. Murad, F. Laffir, C. Dickinson and E. Dempsey, *Nanoscale* 2011, 3, 3334–3349.
- X.L. Peng, Y.C. Zhao, D.H. Chen, Y.F. Fan, X. Wang and J.N. Tian, *Electrochim. Acta* 2014, 136, 292–300.
- H.J. Huang and X. Wang, *J. Mater. Chem. A* 2014, 2, 6249–6670.
- C.C. Hung, C. Li and G.Q. Shi, *Energy Environ Sci.* 2012, 5, 8848–8868.
- X. Zhao, M. Yin, L. Ma, L. Liang, C.P. Liu, J.H. Liao, T.H. Lu and W. Wang, *Energy Environ Sci.* 2011, 4, 2736–2753.
- N. Tian, Z.Y. Zhou, S.G. Sun, Y. Ding and Z.L. Wang, *Science* 2007, 316, 732–735.
- H.A. Gasteiger and N.M. Markovic, *Science* 2009, 342, 48–49.
- V.R. Stamenkovic, B. Fowler, B.S. Mun, G. Wang, P.N. Ross, C.A. Lucas and N.M. Markovic, *Science* 2007, 315, 493–496.
- S.C. Hall, V. Subramanian, G. Teeter and B. Rambabu, *Solid State Ionics* 2004, 175, 809–813.
- C. Bianchini and P.K. Shen, *Chem. Rev.* 2009, 109, 4183–4206.
- C.W. Xu, P.K. Shen and Y.L. Liu, *J. Power Sources* 2007, 164, 527–531.
- J.Q. Ye, J.P. Liu, C.W. Xu, S.P. Jiang and Y.X. Tong, *Electrochem. Commun.* 2007, 9, 2760–2763.
- L.Z. Li, M.X. Chen, G.B. Hung, N. Yang, L. Zhang, H. Wang, Y. Liu, W. Wang and J.P. Gao, *J. Power Sources* 2014, 263, 13–21.
- Y.Y. Feng, Z.H. Liu, Y. Xu, P. Wang, W.H. Wang and D.S. Kong, *J. Power Sources* 2013, 232, 99–105.
- E.A. Monyoncho, S. Ntais, F. Soares, T.K. Woo and E.A. Baranova, *J. Power Sources* 2015, 287, 139–149.
- V. Bambagioni, C. Bianchini, A. Marchionni, T. Filippi, F. Vizza, J. Teddy, P. Serp and M. Zhiani, *J. Power Sources* 2009, 190, 241–251.

- 19 J. Qi, J.B. Wu, H. Zhang, Y.Y. Jiang, C.H. Jin, M.S. Fu, H. Yang and D. Yang, *Nanoscale* 2014, 6, 7012–7018.
- 20 S.S. Shendage, A.S. Singh and J.M. Nagarkar, *Mater. Res. Bull.* 2015, 70, 539–544.
- 21 Y.C. Zhao, X.L. Yang, J.N. Tian, F.Y. Wang and L. Zhan, *Int. J. Hydrogen Energy* 2010, 35, 3249–3257.
- 22 T. Arikan, A.M. Kannan and F. Kadirgan, *Int. J. Hydrogen Energy* 2013, 38, 2900–2907.
- 23 S. Guo, X. Zhang, W. Zhu, K. He, D. Su, A. Mendoza-Garcia, S.F. Ho, G. Lu and S. Sun, *J. Am. Chem. Soc.* 2014, 136, 15026–15033.
- 24 S. Sharma and B.G. Pollet, *J. Power Sources* 2012, 208, 96–119.
- 25 L. Calvillo, V. Celorrio, R. Moliner and M.J. Lázaro, *Mater. Chem. Phys.* 2011, 127, 335–341.
- 26 V. Celorrio, M.G. Montes de Oca, D. Plana, R. Moliner, M.J. Lázaro and D. J. Fermín, *J. Phys. Chem. C* 2012, 116, 6275–6282.
- 27 B.P. Vinayan, R. Nagar, N. Rajalakshmi and S. Ramaprabhu, *Adv. Funct. Mater.* 2012, 22, 3519–3526.
- 28 C. Paoletti, A. Cemmi, L. Giorgi, R. Giorgi, L. Piloni, E. Serra and M. Pasquali, *J. Power Sources* 2008, 183, 84–91.
- 29 Y.Y. Song, Y. Li and X.H. Xia, *Electrochem. Commun.* 2007, 9, 201–205.
- 30 J.J. Zhang, Z.B. Wang, C. Li, L. Zhao, J. Liu, L.M. Zhang and D.M. Gu, *J. Power Sources* 2015, 289, 63–70.
- 31 A. Safavi, A. Abbaspour and M. Sorouri, *J. Power Sources* 2015, 287, 458–464.
- 32 X. Zhang, B. Zhang, X.D. Li, L.X. Ma and J.W. Zhang, *Int. J. Hydrogen Energy* 2015, 40, 14416–14420.
- 33 Y. Zhang, L. Jiang, H. Li, L.Z. Fan, W.P. Hu, C.R. Wang, Y.F. Li and S.H. Yang, *Chem. Eur. J.* 2011, 17, 4921–4926.
- 34 X. Zhang and L.-X. Ma, *J. Power Sources* 2015, 286, 400–405.
- 35 X. Zhang, L.-X. Ma and Y.-C. Zhang, *Electrochim. Acta* 2015, 177, 118–127.
- 36 X. Zhang, B. Zhang, D.Y. Liu and J.L. Qiao, *Electrochim. Acta* 2015, 177, 93–99.
- 37 H.Y. Na, L. Zhang, H.X. Qiu, T. Wu, M.X. Chen, N. Yang, L.Z. Li, F.B. Xing and J.P. Gao, *J. Power Sources* 2015, 288, 160–167.
- 38 H. Zhang, C.-D. Gu, M.-L. Huang, X.-L. Wang and J.-P. Tu, *Electrochem. Commun.* 2013, 35, 108–111.
- 39 S. Park and R.S. Ruoff, *Nature Nanotech.* 2009, 4, 217–224.
- 40 J.S. Bunch, A.M. Zande, S.S. Verbridge, C.W. Frank, D.M. Tanenbaum, J.M. Parpia, H.G. Craighead and P.L. McEuen, *Science* 2007, 315, 490–492.
- 41 J. Liu, Y.H. Xue, M. Zhang and L.M. Dai, *MRS Bulletin* 2012, 37, 1265–1272.
- 42 X. Yan, B.S. Li, X. Cui, Q.S. Wei, K. Tajima and L.S. Li, *J. Phys. Chem. Lett.* 2011, 2, 1119–1124.
- 43 C. Matteri, G. Eda, S. Agnoli, S. Miller, K.A. Mkhoyan, O. Celik, D. Mastrogianni, G. Granozzi, E. Garfunkel and M. Chhowalla, *Adv. Funct. Mater.* 2009, 19, 2577–2583.
- 44 G. Eda, Y.Y. Lin, C. Mattevi, H. Yamaguchi, H.A. Chen, L.S. Chen, C.W. Chen and M. Chhowalla, *Adv. Mater.* 2010, 22, 505–509.
- 45 S. Stankovich, D.A. Dikin, G.H.B. Dommett, K.M. Kohlhaas, E.J. Zimney, E.A. Stach, R.D. Piner, S.T. Nguyen and R.S. Ruoff, *Nature* 2006, 442, 282–286.
- 46 J.W.S. Hummers and R.E. Offeman, *J. Am. Chem. Soc.* 1958, 80, 1339.
- 47 L.J. Cote, F. Kim and J.X. Huang, *J. Am. Chem. Soc.* 2009, 131, 1043–1049.
- 48 L.Y. Chen, H. Guo, T. Fujita, A. Hirata, W. Zhang, A. Inoue and M.W. Chen, *Adv. Funct. Mater.* 2011, 21, 4364–4370.
- 49 W. Wang, S. Ji, H. Wang and R.F. Wang, *Fuel Cells* 2012, 6, 1129–1133.
- 50 M.A. Matin, J.H. Jang and Y.U. Kwon, *J. Power Sources* 2014, 262, 356–363.
- 51 G. Xiao, *Fuel Cell Technology*, Publishing House of Electronics Industry, Beijing, 2009, 45–46.
- 52 N. Tian, Z.-Y. Zhou and S.-G. Sun, *Chem. Commun.* 2009, 12, 1502–1504.
- 53 M.E. Scofield, C. Koenigsmann, L. Wang, H. Liu and S.S. Wong, *Energy Environ. Sci.* 2015, 8, 350–363.

Anchoring ternary CuFePd nanocatalysts on reduced graphene oxide to improve the electrocatalytic activity for the methanol oxidation reaction

Xuan Zhang*, Jia-Wei Zhang†, Bei Zhang†



A ternary CuFePd/rGO electrocatalyst was facilely developed and exhibited improved performance in comparison with binary CuPd/rGO and FePd/rGO, as well as Pd/rGO, respectively.